Periodic Forcing of the Swift-Hohenberg Equation in Time

Punit Gandhi,* Cédric Beaume, and Edgar Knobloch

Department of Physics, University of California, Berkeley CA 94720, USA

(Dated: May 7, 2014)

Abstract

Systems with a periodic forcing in time abound! We use the generalized Swift-Hohenberg equation with a quadratic-cubic nonlinearity as test-bed for studying localized pattern formation in such systems with a periodic forcing in time. We apply a sinisiodal linear forcing to the SHE and study the dependence of localization on the amplitude, oscillation period, and offset of the forcing. As one might expect, the region of existence of stable localized solutions dramatically decreases as the system is "jiggled." The parameter space within the pinning region of the constant forcing case, however, is partitioned into regions of growth, stability, and decay with an unexpected structure when large oscillations are applied.

* punit_gandhi@berkeley.edu

I. INTRODUCTION

Time-dependent forcing can be critical to the understanding of pattern formation in certain systems. The Earth's rotation and orbit provide a periodic forcing for many systems on Earth. Some other stuff....

The Swift–Hohenberg equation [1] (SHE) serves as a model for pattern formation in a broad range of physical systems []. The existence, structure, and stability of localized solutions within the SHE has been studied in great detail [2–4]. This equation, which takes the form

$$u_t = ru - \left(1 + \partial_x^2\right)^2 u + N[u], \tag{1}$$

describes the dynamics of a real field u over one spatial dimension in time, where N is some nonlinear function of u. We have rescaled the equation so that the critical wavenumber that defines the natural wavelength of the patterned state is unity. We will be interested in two possible choices of N, namely $N_{23}[u] = bu^2 - u^3$ and $N_{35}[u] = bu^3 - u^5$. The strength of the linear forcing term r and the strength of the quadratic/cubic nonlinearity b are left as parameters of the system.

We consider the case when the forcing is no longer constant in time, namely $r \to r_0 + \delta r \sin \omega t$. Pattern formation in ecological systems that are periodically forced by the seasons or the daily variations in insolar flux are one example of a physical motivation for considering this kind of system []. Other physical systems that might be described by such a periodically forced model include ... []. Furthermore, oscillations that effectively create and destroy attractors have been shown to produce new "ghost" attractors that do not exist in the time-independent system for any value of the parameter[]. While this has been done for the case of simple oscillators, the present work provides an extension of these observations to higher dimensions.

All simulations in time used periodic boundary conditions and a domain of $L = 80\pi$ (e.g. 40 characteristic wavelengths), unless otherwise noted. A 4th order exponential time differencing scheme[5] was used to step forward in time while spectral methods on a grid of 1024 points were used for the spatial calculations. Steady state solutions of the constant forcing case were computed by numerical continuation using AUTO [6].

We first recount the relevant details of the original Swift-Hohenberg equation before discussing some numerical results and theoretical analysis of the periodically forced case.

We begin by examining the effect of small oscillations on the growth and decay of slightly unstable localized solutions, and then move to large oscillations that extend through and beyond the pinning region of the constant forcing case. Finally, discuss the persistence of a localized defect state that would be unstable without the oscillations before concluding with a summary of the results and an outlook on future work.

A. motivation for periodic time forcing in pattern formation

B. Description for SHE

C. Numerical Methods

D. paper outline

II. CONSTANT FORCING IN TIME

Here we will describe the structure and some relevant properties of the solutions of SHE with a constant forcing. Because Eq. **??** can be written in terms of the variation of a free energy (or Lyaponov functional)

$$\mathcal{F}[u] = -\frac{1}{L}\int_{-L/2}^{L/2} \tfrac{1}{2}ru^2 - \tfrac{1}{2}\left[(1+\partial_x^2)u\right]^2 - M[u]\,dx \tag{2}$$

where $M'[u] = N[u]$, the solution will approach a steady state in time on the periodic domain that corresponds to a local minimum of this free energy. If we consider the space of steady-state solutions, we find that a periodic solution u_p ($u_p(x) = u_p(x+2\pi)$), is formed from a bifurcation at $r = 0$ where the trivial solution $u_0 = 0$ changes stability. On a finite domain, the domain size and boundary conditions will determine a series of periodic solutions of differing period that emerge from the trivial branch for $r > 0$ as it becomes more and more unstable. We will focus on the case that the periodic branches emerges subcritically and the trivial branch becomes unstable in time for $r > 0$. For a suitable choice of b ($b = 1.8$, for example), this bifurcation structure along with a pinning region that forms around the Maxwell point ($\mathcal{F}[u_p] = \mathcal{F}[u_0] = 0$) where the energy between the trivial and periodic states is sufficiently close that stable localized states formed from fronts between the two can also

exist. A bifurcation diagram of the steady state solutions (Fig. 1, from J. Burke et et al) shows the trivial state, the periodic state, and localized solution branches within the pinning region.

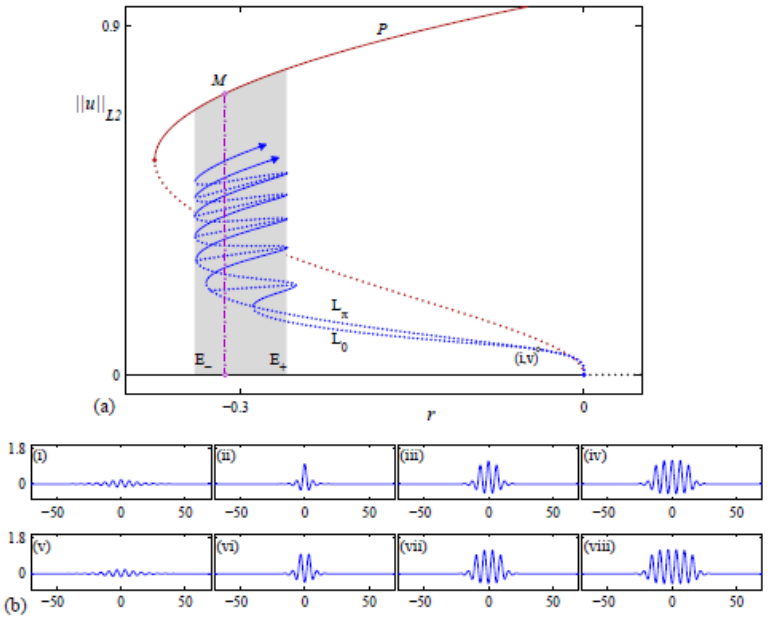

FIG. 1: This figure was taken from Burke[] (a) Bifurcation diagram showing the snakes-and-ladders structure of localized states. Away from the origin the snaking branches L_0 and L_- are contained within the snaking region (shaded) betweenE_- and E_+, where $r(E_-) \approx -0.3390$ and $r(E_+) \approx -0.2593$. Solid (dotted) lines indicate stable (unstable) states. In addition, the Maxwell point M, occurring at $r(M) \approx -0.3128$ is indicated with a vertical dash-dot line. The saddle node bifurcation that creates the stable periodic state occurs at $r < r(SN_P) \approx -0.3744$, defining the left edge of the bistability region. We will also find it useful to define the center of the snaking region C, which corresponds to the forcing parameter $r(C) \approx -0.2992$. (b) Sample localized profiles $u(x) : (i - iv)$ lie on L_0, near onset and at the 1st, 3rd, and 5th saddle-nodes from the bottom, respectively; (v-viii) lie on L_-, near onset and at the 1st, 3rd, and 5th saddle-nodes, respectively. Parameters: $b = 1.8$.

For our choice of parameter $b = 1.8$ and a domain size $L = 80\pi$, the trivial solution is stable for $r < 0$ and becomes unstable as as the periodic solution is created through

a bifurcation at $r = 0$. As we are looking at the subcritical case, we see a saddle-node bifurcation of the periodic branch where it gains stability at SN_P. Thus we have only a stable trivial solution for $r < r(SN_P) \approx -0.3744$. At this point, a stable periodic solution is created but is energetically unfavorable to the trivial state. For $r(E_-) < r < r(E_+)$, we have a zoo of localized solutions (including an entire sequence of stable localized solutions on each snaking branch) that exist in addition to the stable trivial and periodic solutions. We note that within this region, $r(M)$ indicates the transition from the trivial state being energetically favorable to the periodic state becoming energetically favorable. We will also find it useful to define the center of the snaking region C, which corresponds to the forcing parameter $r(C) \approx -0.2992$. Between $r(E_+)$ and $r = 0$, we again have only the periodic solution and the trivial solution as stable but with the periodic solution now more energetically favorable. Finally, for $r > 0$, the trivial solution looses stability and only the periodic solution remains as stable. We note that other stable solutions exist (e.g. the flat, nonzero solutions created at the transcritical bifurcation at $r = 1$) but that they have not been found to play a role in our region of interest with our current choice of parameters (e.g. $b = 1.8$).

Solutions near steady-state have also been considered. Burke and Knobloch [2] have shown that near the pinning region (e.g. for $r = r(E_\pm) \pm \delta$ where $\delta << 1$), a localized solution that was stable at the edge of the pinning region will move towards the more energetically favorable of the trivial and the periodic state at a constant rate. Above the snaking region, for example, a localized solution will nucleate periods of the pattern in quick bursts with some longer transition time $T_{\text{nuc}} \propto \delta^{-1/2}$ in between each nucleation event.

An numerical example of this on a domain of 40 periods of the characteristic wavelength is shown in Fig. **??**. A localized solution that is stable for $r = r(E_+)$ is initialized above the snaking region (e.g. $r = r(E_+)+?\delta?$) and allowed to grow until it fills the domain. We note that it grows to a solution containing 39 periods, and a corresponding numerical continuation calculation produces a snaking branch of steady state solutions that emerges as a secondary bifurcation from a 40 period solution but reconnects to a 39 period solution. This phenomenon has been explained [7] in terms of the Eckhaus instability for the case of the steady state solutions. Intuitively, the wavelength of the localized solution is slightly longer than the characteristic wavelength of the solution because the more energetically favorable periodic state wants to expand into the trivial state. As the localized solution grows to a domain filling size, it finds that there isn't enough room to nucleate the 40th

wavelenth of the solution. Because we are outside of the region that is Eckhaus stable, the wavelenth instead grows to fill the domain with 39 periods.

We can see from Fig. 2 that the time from one nucleation event to the next is approximately ??, though the last nucleation event seems to take a bit longer.

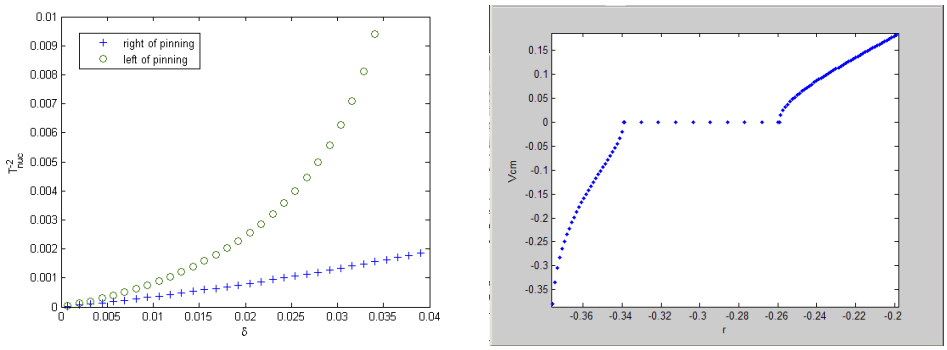

(a) (b)

FIG. 2: Simulation of the SHE with N_{23} with $b = 1.8$ show (a) $1/T_{nuc}^2$, where T_{nuc} is the time between nucleation/decay events, as a function of distance from the edge of the pinning region δ, and (b) the front speed as a function of the forcing parameter. We note that the initial solution used in these simulations was on a saddle node bifurcation of snaking branch at the closest edge of the pinning region.

We show the results of simulations for our parameters (Fig. 2) to numerically confirm the $T_{nuc} \propto \delta^{-1/2}$ law and locate the region of validity. We also show a graph of the front speed (calculated as $2\pi/T_{nuc}$) as a function of r_0 for the constant forcing case. It is clear from these graphs, that the front moves faster to the left of pinning region in the parameter regime we are looking at. We also note that beyond δ of about 0.036, the decays of periods of the solutions to the left of the pinning region are no longer clearly separated by a period of slow change in the solution. Beyond this value, instead of depinning, the solution approaches the trivial stat by an overall amplitude decay.

A. free energy and SHE

B. bistability and maxwell point

C. snakes and ladders structure within pinning region

D. front speed just outside pinning region

E. Eckhaus instability and connection of snaking branch to different period periodic branch

F. Description of simple toy model of SHE and nucleations??

III. PERIODIC FORCING IN TIME

As a proxy for the location of the front, we track the front of solution in terms of its first moment on half the domain:

$$X_{cm} = \frac{1}{||u||} \int_0^{L/2} x u^2 dx \tag{3}$$

where

$$||u|| = \int_0^{L/2} |u|^2 dx \tag{4}$$

This give half the distance from the center of the domain to the edge of a localized solution. The speed is then defined by $V_{cm} = dX_{cm}/dt$, and is really half the speed of the front.

We note that changing the phase of the oscillation in the forcing (e.g. $\rho \to -\rho$) does not seem to affect the stable region in this graph. There is a symmetry of the equation $\rho \to -\rho$, and $t \to -t$.

n an attempt to provide some context to the results in the we define the "oscillating Maxwell point" in the oscillation center r_0 where the average free energy along an oscillation of solution that is stable in time and periodic in space equals the free energy of the trivial solution (e.g. zero). For the parameter $\rho = 0.1$, we find this value to be shifted to the left by about 0.5 from the Maxwell point of the constant forcing case to $r_* \approx -0.318$ (Fig. **??**. The average free energy of oscillation does not have a strong dependence on the oscillation frequency, except that the stable oscillating solution does not exist for very slow frequencies in some cases. This is because the oscillations take the system well beyond the saddle-node where the stable periodic solution of the constant forcing case is created.

Figures 3 and 4 plot various phase space slices of the orbits of the stable cases detailed in the above figures in hopes of gaining some insight into the dynamics.

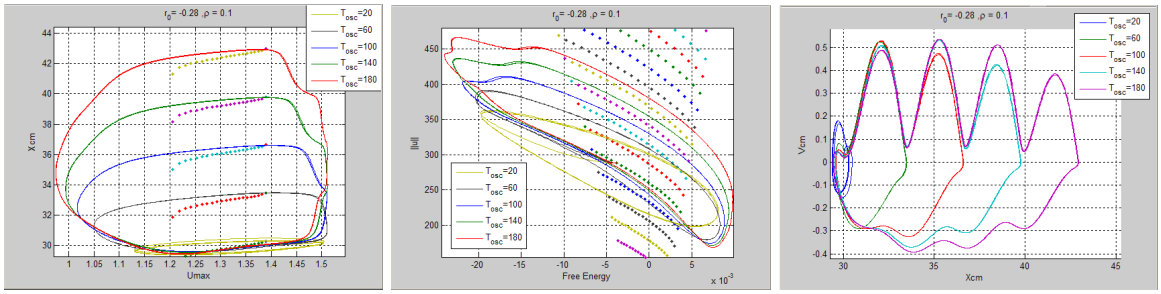

FIG. 3: Various phase space slices of solutions along $r_0 = -.28$ with $\rho = -0.1$ that are periodic in time. (a)The maximum height of the solution vs the position of the front. the motivation here was to graph the length and heigth of the solution to give some sense of its size. (b) The free energy of the solution vs the L2 norm. (c) the phase space of the front, the postion of the front vs its speed.

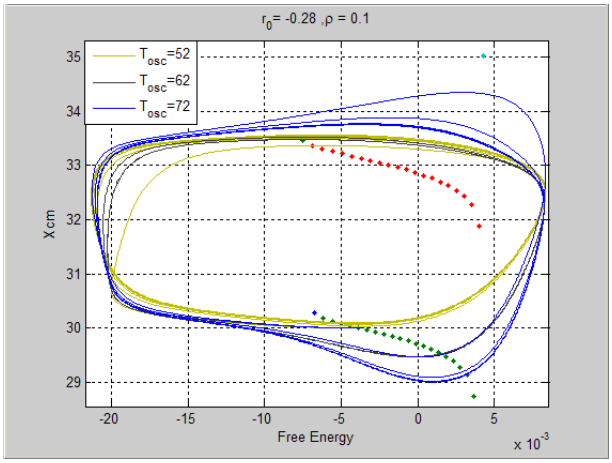

FIG. 4: Trajectories in phase space of an orbit at the edges and center of the stable region in parameter space.

A. schematic of solution structure and regions will oscillate through

B. description of some behaviors exhibited (growing, decaying ,stable, etc..)

C. descrption of ways to visualize solutions (Xcm,Vcm, slices of phase space we will use, etc..)

IV. EFFECT OF SMALL OSCILLATIONS ON THE FRONT SPEED NEAR THE EDGE OF THE PINNING REGION

A. graph of numerical results - we don't really have this yet

B. asymptotic calculation and comparison to numerical result

Following Burke's calculation for the standard SHE to find the time between nucleation events, we derive an equation that estimates the effects of small, slow oscillations on the depinning process. We will perform this calculation just to the right of r_+, the right edge of the pinning region of the constant forcing case (e.g. $r \to r_+ + \epsilon^2\delta$). Note that the exact same procedure could be used to find the time between decay events just to the left of the pinning region. We will assume small (e.g. $\rho \to \epsilon^2\rho$), slow oscillations (e.g. $\omega \to \epsilon\omega$) so that the deviation from Burke's calculation will be small in this case. The equation, in this limit becomes

$$u_t = \left(r_+ + \epsilon^2(\delta + \rho \sin \epsilon\omega t)\right) u - \left(1 + \partial_x^2\right)^2 u + bu^2 - u^3, \tag{5}$$

where r_+ is the right edge of the pinning region when $\rho, \delta = 0$. Because we are near the pinning region, we can assume the dynamics will be slow and will define the slow timescale $\tau = \epsilon t$ and corresponding time derivative $\partial_t \to \epsilon\partial_\tau$. After writing u as an asymptotic series, $u = u_0 + \epsilon u_1 + \epsilon^2 u_2 + ...$, we can write out the equation order by order in ϵ. At leading order, we have

$$r_+ u_0 - \left(1 + \partial_x^2\right)^2 u_0 + bu_0^2 - u_0^3 = 0, \tag{6}$$

and can thus pick u_0 to be a localized solution at a saddle-node bifurcation of the snaking branch. Thus u_0 is stationary in time, but only marginally stable. Going on to order $\mathcal{O}(\epsilon)$, we get

$$\partial_\tau u_0 = r_+ u_1 - \left(1 + \partial_x^2\right)^2 u_1 + 2bu_0 u_1 - 3u_0^2 u_1 \tag{7}$$

Since we have chosen u_0 to be stationary in time, u_1 must be a zero eigenvector of the SHE linearized about the solution a the saddle-node of the snaking branch. Just as in Burke's calculation, the relevant eigenvector is the one that corresponding to the direction that adds periods to the localized solution (u_{amp}) and it conveniently has an eigenvalue of 0 since we are right on the saddle-node. Thus we can write the correction in the form $u_1 = a(\tau)u_{\text{amp}}$. We must go on order $\mathcal{O}(\epsilon^2)$ to determine a. At this order, the equation is

$$\partial_\tau u_1 = r_+ u_2 - \left(1 + \partial_x^2\right)^2 u_2 + 2bu_0u_2 - 3u_0^2u_2 + (\delta + \rho \sin \omega\tau)u_0 + bu_1^2 - 3u_0u_1^2 \tag{8}$$

Because the linear operator acting on u_2 is self-adjoint and u_{amp} is in it's nullspace, we use this equation to obtain the following solvability condition that determines a.

$$\alpha_1 \dot{a} = \alpha_2(\delta + \rho \sin \omega\tau) + \alpha_3 a^2, \tag{9}$$

where

$$\begin{aligned} \alpha_1 &= \int_0^L u_{\text{amp}}(x)^2 dx \\ \alpha_2 &= \int_0^L u_{\text{amp}}(x)u_0(x)dx \\ \alpha_3 &= \int_0^L u_{\text{amp}}(x)^3(b - 3u_0(x))dx \end{aligned} \tag{10}$$

Under the proper rescaling of parameters, the equation becomes

$$\dot{a} = \delta + \rho \sin \omega\tau + \alpha a^2. \tag{11}$$

V. STABILITY, GROWTH, AND DECAY OF LOCALIZED SOLUTIONS UNDER LARGE OSCILLATIONS

A. Stable oscillations of the solution

1. *stable region for* $\rho = .1, .8, .6$

2. ρ *vs* r_0, *Tosc=100*

B. Growth and decay

1. *big detailed figure of nucleations per oscillation*

2. *stability lines and avoided crossings?*

3. *simple model interpretaion*

C. some asymptotic calculations???

VI. PERSISTENCE OF DEFECTS DUE TO OSCILLATIONS

Using an oscillation with a period of 50 and centered about $r_0 = -0.27$ and amplitude of $\rho = 0.1$, we can see the trajectory taken by the initial localized solution as it approaches a domain filling one (Fig. 5). The solution grows by nucleating a period on each front at each oscillation of the forcing parameter. This happens until the solution reaches 39 periods, at which point it seems to get stuck. Eventually it fills the domain with a 40 period solution. This is in contrast to the case with a constant forcing that grows into the domain with a 39 period solution.

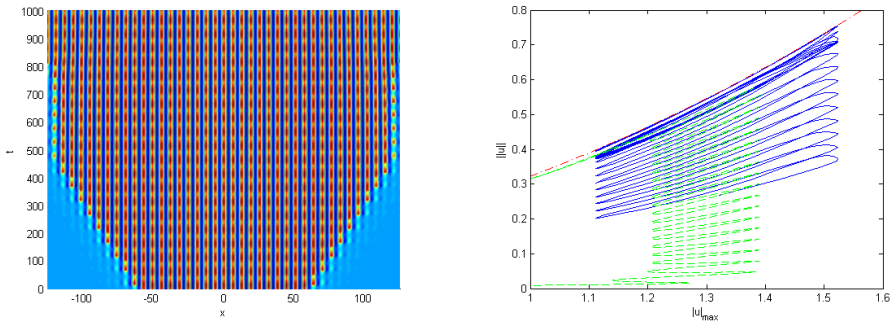

(a) (b)

FIG. 5: Oscillations of the forcing parameter in and out of the snaking region. The forcing parameter as a function of time is given by $r \to -0.27 + 0.1 \sin 2\pi t/50$. The solution (a) grows in time, eventually filling the domain and the corresponding trajectory along the max value - L2 norm phase space slice (b) shows the path taken as it passes in and out of the snaking region .

A. show solutions of quasistable defect connecting to both 39 and 40 period solution as well as stable defect

B. graph of regions where for each case

C. Some kind of explanaition (Eckaus instability and delayed bifurcations?)

VII. CONCLUSION

A. summarize results

B. future directions

---

[1] J Swift and Pierre C Hohenberg, "Hydrodynamic fluctuations at the convective instability," Physical Review A **15**, 319 (1977).

[2] John Burke and Edgar Knobloch, "Localized states in the generalized swift-hohenberg equation," Physical Review E **73**, 056211 (2006).

[3] John Burke and Edgar Knobloch, "Snakes and ladders: localized states in the swift–hohenberg equation," Physics Letters A **360**, 681–688 (2007).

[4] John Burke and Edgar Knobloch, "Homoclinic snaking: structure and stability," Chaos: An Interdisciplinary Journal of Nonlinear Science **17**, 037102–037102 (2007).

[5] SM Cox and PC Matthews, "Exponential time differencing for stiff systems," Journal of Computational Physics **176**, 430–455 (2002).

[6] Eusebius J Doedel, "Auto: A program for the automatic bifurcation analysis of autonomous systems," Congr. Numer **30**, 265–284 (1981).

[7] Alain Bergeon, J Burke, E Knobloch, and I Mercader, "Eckhaus instability and homoclinic snaking," Physical Review E **78**, 046201 (2008).